Recombination of Aromatic Radicals with Molecular Oxygen

Feng Zhang, André Nicolle, Lili Xing, Stephen J Klippenstein

*Title Page

Recombination of Aromatic Radicals with Molecular Oxygen

Feng Zhang,[1,2,] André Nicolle,[2,3] Lili Xing,[1] and Stephen J. Klippenstein[2]*

[1] National Synchrotron Radiation Laboratory, University of Science and Technology of China, Hefei, Anhui 230029, P. R. China

[2]Chemical Sciences and Engineering Division, Argonne National Laboratory, Argonne, IL 60439, USA

[3] IFP Energies Nouvelles, 1-4 Avenue de Bois-Préau, 92852 Rueil-Malmaison Cedex, France

Corresponding Authors:

Feng Zhang

National Synchrotron Radiation Laborator, University of Science and Technology of China, Hefei, Anhui 230027, P. R. China

Tel: +86-551-63607923

Fax: +86-551-65141078

E-mail: feng2011@ustc.edu.cn

Colloquium:

REACTION KINETICS

Word Count (Method 1):

The total word count (exclusive of title page, abstract) is: **5774** words

Word Count (was performed from automatic counting function in MS Word plus Figs/Table/References)

Abstract: 117 words, not included in word count

Main text: **3546** words

References: **629** words (34 references)

Tables: **0** words (0 table)

Equations: **30** words (2 equations, single column)

Figures: **1569** words (8 figures with captions)

Figure	Column	Height/mm	Word Count
1	double	83	411
2	single	85	209
3	single	49	130
4	single	51	134
5	single	53	138
6	single	52	136
7	single	52	136
8	single	46	123
Captions			150

Total: 5774 words

Supplementary Material: one supplementary material is available.

Recombination of Aromatic Radicals with Molecular Oxygen

Feng Zhang,[1,2,] André Nicolle,[2,3] Lili Xing,[1] and Stephen J. Klippenstein[2]*

[1] National Synchrotron Radiation Laboratory, University of Science and Technology of China, Hefei, Anhui 230029, P. R. China

[2]Chemical Sciences and Engineering Division, Argonne National Laboratory, Argonne, IL 60439, USA

[3] IFP Energies Nouvelles, 1-4 Avenue de Bois-Préau, 92852 Rueil-Malmaison Cedex, France

Abstract:

The addition of molecular oxygen to hydrocarbon radicals yields peroxy radicals (ROO), which are crucial species in both atmospheric and combustion chemistry. For aromatic radicals there is little known about the recombination kinetics, especially for the high temperatures of relevance to combustion. Here, we have employed direct CASPT2 based variable reaction coordinate transition state theory to predict the high pressure recombination rates for four prototypical aromatic hydrocarbon radicals: phenyl, benzyl, 1-naphthyl, and 2-naphthyl. The variation in the predicted rates is discussed in relation to their molecular structure. The predicted rate coefficients are in reasonably satisfactory agreement with the limited experimental data and are expected to find utility in chemical modeling studies of PAH growth and oxidation.

Keywords: hydrocarbon peroxy radicals; aromatic radicals; recombination reactions; quantum chemical calculations; variable reaction coordinate transition state theory

1. Introduction

Aromatic compounds contribute greatly to the emission of polycyclic aromatic hydrocarbons (PAH) and soot and are key precursors to the formation of tropospheric ozone and secondary organic aerosols [1,2]. As such, an accurate understanding of their oxidation kinetics is crucial to the modeling of both atmospheric and combustion chemistry [3-6]. In the low temperature oxidation environment, ROO chemistry is of direct relevance to the chain reactions that ultimately lead to autoignition [4,6]. The recombination reaction between hydrocarbon radicals and oxygen molecule is a significant source of ROO, triggering the subsequent ROO chemistry.

Combustion modeling studies on the oxidation of aromatic hydrocarbon fuels such as benzene, toluene, and naphthalene (see, e.g, [7-9]) have generally estimated the kinetic data for the fuel radical R + O_2 reaction from experience or via extrapolation of relatively low-temperature experimental measurements [10-12]. For phenyl, measurements of Yu et al. [10] over the 297-473 K temperature range suggest that the O_2 recombination rate constant decreases with temperature, while Schaugg et al.'s measurements showed a positive temperature dependence at slightly higher temperatures (418-815 K) [13]. For benzyl, both Hoyermann et al. [14] and Nelson et al. [15] observed no temperature dependence over the 243–373 K range, while Fenter et al. indicate a significant decline with increasing temperature at analogous temperatures (298-398 K) [11]. Only Park et al. have measured the rate constant for 2-naphthyl, finding a modest decrease over the 299-444 K temperature range. These discrepancies in the observed temperature behavior add to the uncertainty in any attempted extrapolations to combustion temperatures.

There is also discordancy in recent theoretical predictions of the temperature dependence for aromatic radical + O_2 recombination kinetics. The canonical variational transition state theory (VTST) calculations of da Silva et al. [16] predict that the rate coefficient for phenyl + O_2 should

decrease by about a factor of 4 over the 300-2000 K temperature range. In contrast, the very recent variable reaction coordinate transition state theory (VRC-TST) [17] calculations of Kislov et al. [18] predict that for phenyl, 1- and 2-naphthyl radicals the O_2 recombination rate constant should rise over the 1500-2500 K range, in qualitative accord with the results of Schaugg et al. [13,18].

In this work, the O_2 recombination reaction was studied for four representative aromatic hydrocarbon radicals: phenyl, benzyl, 1- and 2-naphthyl radicals. The radical characteristics of triplet O_2 result in a barrierless minimum energy path for its addition to radicals [19,20]. Prior applications of the VRC-TST approach, such as the recent application to the closely related $C_2H_3 + O_2$ addition reaction [19], have amply demonstrated its ability to accurately predict the rate coefficients for such barrierless radical-radical reactions.

Hence, the present analysis employs VRC-TST as in the work of Kislov et al. [18], but proceeds beyond it in a variety of ways. Their approximate representation of the transitional mode interaction potential is replaced here with direct CASPT2 determinations. Furthermore, accurate estimates of the minimum energy path (MEP) energies are obtained through multireference based evaluations of the spin-splitting combined with coupled-cluster based evaluations for the high spin quartet state, as in the $C_2H_3 + O_2$ study.

2. Methodology

2.1 Kinetic theory

The key assumption in VRC-TST is the separation of the “conserved” and “translational” modes in the transition state region of the potential. The conserved modes, which correspond to the vibrational modes of the reacting fragments, are treated as quantized harmonic oscillators. The transitional modes correspond to the remaining modes, which describe the rotational and translational motions of

the two reacting fragments. The essential advantage of the VRC-TST approach is its quantitative treatment of the full coupling and anharmonicity of the transitional modes through Monte Carlo integration over the coordinate space degrees of freedom in the classical phase space representation for the reactive flux for a variable set of reaction coordinates.

The variability of the reaction coordinate in VRC-TST is achieved by choosing a set of pivot points whose locations and separations determine the transition state dividing surface. The rate constant is then minimized with respect to both the pivot point locations and separation distances. For the four R + O_2 reactions studied in this work, two sets of dividing surfaces were used. The first set employs center-of-mass (CoM) pivot points, which are appropriate for large separations, while the second set employs orbital centered pivot points, which are appropriate for shorter separations.

A separate 6-point-mesh with a variable grid spacing of 1.0–4.0 au was used for the larger separations (9.0-21.0 au) where the CoM pivot points are used. A 12-point-mesh with finer grids (0.3-1.0 au) was used for the shorter separations (3.8-9.0 au) with orbital centered pivot points. For the orbital centered pivot points, their displacement from the bonding atoms was varied from 0.5 to 1.5 au, with a step size of 0.5 au. With the preferred E,J-resolved VRC-TST, which was employed here, the reaction coordinate minimizations are performed for each energy, E, and total angular momentum J. A dynamical correction (0.85) was used for the final rate coefficients.

2.2 Quantum chemical calculations

The implementation of the VRC-TST approach requires accurate interfragment interaction energies for ~10^4 configurations for each reaction. The program VaReCoF [21], which was used in the present work, allows for the evaluation of these interactions on-the-fly, with direct calls to ab initio electronic structure methods. The complete active space self-consistent field theory with

second-order perturbation (CASPT2) [22] method combined with the cc-pVDZ basis set efficiently yields interaction energies of suitable accuracy [19,20]. Here, a 7-electron 5-orbital (7e,5o) active space was chosen to optimize the MEP for all four R + O_2 reactions. This space correlates with the two pairs of O-O π and π^* orbitals, and the radical orbital of R. An ionization potential-electronic affinity (IPEA) shift of 0.25, was introduced into the CASPT2 calculations [23].

The CASPT2/cc-pVDZ energy computed for each sampled configuration is corrected by an orientationally independent factor [$\Delta V_{tot}(R_{CO})$], where R_{CO} is the bond length for the incipient CO bond. Since the internal coordinates of the fragments are fixed during the VRC-TST evaluations, this correction factor includes both a relaxation correction and a higher level energy correction. The correction factor was obtained by multi-step composite computations: first, the relaxation correction (ΔV_{relax}) was defined as the energy difference between the MEP built by rigid and relaxed scanning at the CASPT2(7e,5o)/cc-pVDZ level; second, along the MEP, CASPT2 calculations were performed with the cc-pVTZ and cc-pVQZ basis sets, and the energies were extrapolated to the complete basis set limit (CBS) [24]. A basis set correction (ΔV_{basis}) is defined as the CASPT2/CBS to CASPT2/cc-pVDZ energy difference; finally, a method correction (ΔV_{method}) was obtained from CCSD(T)-F12/VDZ-F12 [25,26], MP2-F12/VDZ-F12 [27] and MP2-F12/VTZ-F12 evaluations for the high-spin quartet state:

$$\Delta V_{method} = (V^4_{CCSD(T)-F12/VDZ-F12} + V^4_{MP2-F12/VTZ-F12} - V^4_{MP2-F12/VDZ-F12}) - V^4_{CASPT2/CBS} \quad \text{(E1)}$$

Here the superscript "4" denotes an energy calculated for the quartet state. For phenyl + O_2, the smaller size allowed for additional calculations with larger basis sets, i.e., cc-pVTZ and cc-pVQZ. In summary, the total correction term (ΔV_{tot}) includes three parts, i.e., a geometry relaxation correction, a basis set correction, and a method correction.

For the present method correction, the interaction energy is approximated as the sum of the

CASPT2 calculated quartet-doublet splitting subtracted from the CCSD(T) calculated quartet energy. Note that direct application of CCSD(T) to the doublet state MEP does not yield accurate energies due to the multi-reference nature of the doublet wavefunction in the transition state region. The method correction is effective because the CCSD(T) method accurately treats the high-spin quartet state, while multi-reference treatments of the spin-splitting are more consistent and reliable than corresponding treatments of the absolute interaction energy.

For phenyl and benzyl, we also explored the difference between CASPT2 and multireference configuration interaction MEPs, with the latter performed with (MRCI+Q) and without (MRCI) the Davidson correction. For benzyl, we also explored a CASPT2(13e,11o) active space (which includes the additional (6e,6o) π-space) in order to improve our treatment of the resonance stabilization of the radical.

Reaction enthalpies for benzyl- and naphthyl- + O_2 reactions were computed at the CCSD(T)-F12/VDZ-F12, MP2-F12/VDZ-F12, and MP2-F12/VTZ-F12 levels. The final single point energies were obtained from the expression

$$E = E_{CCSD(T)-F12/VDZ-F12} + E_{MP2-F12/VTZ-F12} - E_{MP2-F12/VDZ-F12} \qquad \text{(E2)}$$

The geometries and zero-point energies for these reaction enthalpy evaluations were obtained with the B2PLYP-D3 density functional method [28], employing the aug-cc-pVDZ basis for C_6H_5OO and C_7H_7OO, and the cc-pVDZ basis for $C_{10}H_7OO$. These density functional theory (DFT) calculations were performed with the Gaussian program [29]. All of the present CASPT2, CCSD(T)-F12, and MP2-F12 calculations were performed with the Molpro program package [30].

3. Results and Discussions

3.1 Structures and reaction enthalpies

The B2PLYP-D3 optimized structures and reaction enthalpies (in brackets) for the ROO complexes arising from the addition of O_2 to phenyl, benzyl, 1- and 2-naphthyl radicals are illustrated in Fig. 1. The Cartesian coordinates for all optimized structures are provided in the Supplemental Material. There are three distinct ROO adducts for the benzyl radical arising from its various resonance configurations. The $C_7H_7O_2$ radical with O_2 added on the methyl branch [i.e., the $C_7H_7O_2$-1 radical shown in Fig. 1 (b1)] is ~19.1 kcal/mol (in the *trans* conformation) more stable than $C_7H_7 + O_2$, while the $C_7H_7O_2$-2 and $C_7H_7O_2$-3 radicals [cf. Fig. 1 (b2) and (b3)] are 5-10 kcal/mol endothermic relative to $C_7H_7 + O_2$. Only the *trans* conformation was considered in the calculations of the one-dimensional corrections for the $C_7H_7O_2$-1 radical.

The orientation of the –OO group in the $C_{10}H_7OO$ complexes has two forms, denoted as $C_{10}H_7OO$–R (right), and $C_{10}H_7OO$–L (left) in Fig. 1 (c) and (d). The steric repulsion arising from the interaction of the –OO group with the nearest H atom is more significant in 1-$C_{10}H_7OO$ than in 2-$C_{10}H_7OO$. Indeed, 1-$C_{10}H_7OO$-R maintains C_s symmetry, while the OOCC dihedral in 1-$C_{10}H_7OO$-L is ~50 degrees. Even with this torsional rotation in 1-$C_{10}H_7OO$-L, the distance from the O to the nearest H is still 0.08 Å shorter than in 1-$C_{10}H_7OO$-R, implying greater steric hindrance in the former configuration. According to the computed reaction enthalpies, 1-$C_{10}H_7OO$-R is 2.2 kcal/mol more stable than 1-$C_{10}H_7OO$-L. In contrast, the –OO orientation has very little effect on the structures or enthalpies for the O_2 addition to form 2-$C_{10}H_7OO$, which is similar to the symmetric C_6H_5OO structure.

The one-dimensional energy profiles required to evaluate ΔV_{tot} were calculated for both 1-$C_{10}H_7OO$-R and 1-$C_{10}H_7OO$-L. The correction energy used in the VRC-TST calculations for 1-$C_{10}H_7 + O_2$ is the mean value of that from the 1-$C_{10}H_7OO$-R and 1-$C_{10}H_7OO$-L MEPs. For 2-$C_{10}H_7OO$ formation only the -R configuration was considered as the energy correction for

2-$C_{10}H_7OO$-L is expected to be nearly identical.

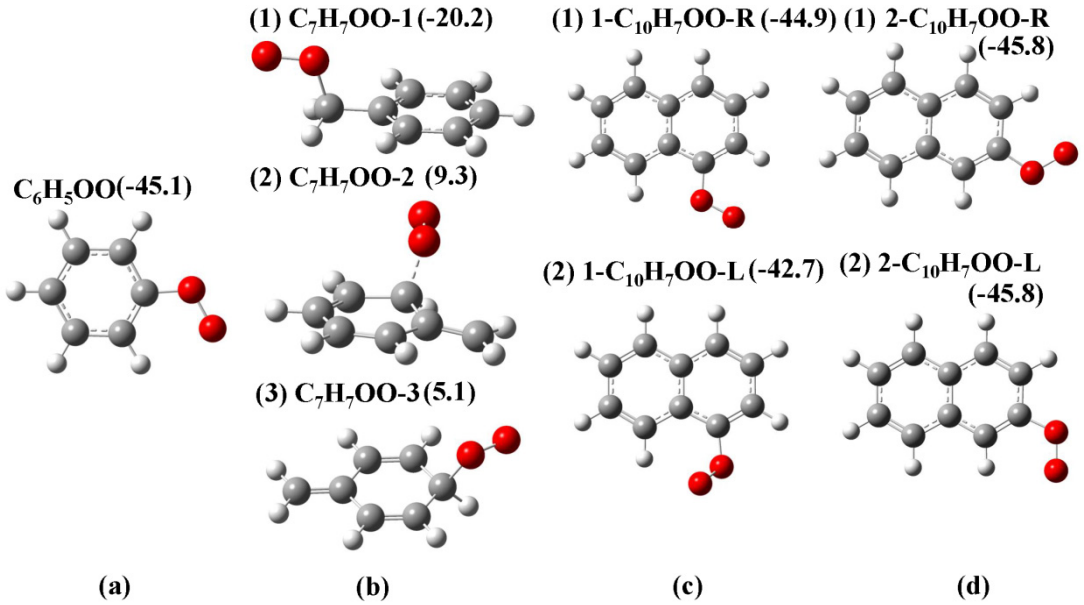

Fig. 1 Optimized ROO complexes for (a) phenyl, (b) benzyl, (c) 1-naphthyl, and (d) 2-naphthyl radicals.

3.2 Phenyl + O_2

Figure 2(a) illustrates the basis set and method dependence of the calculated MEP for the phenyl + O_2 association reaction over R_{CO} distances of 2 to 4 Å, which roughly spans the range of separations for the variational transition state. The potential energy curves were evaluated for geometries along the CASPT2(7,5)/cc-pVDZ relaxed MEP. The CBS correction is seen to decrease the attractiveness at long-range while increasing it at shorter R_{CO}. The M1 method correction (from Eq. (E1)) has only a minor effect on the CASPT2/CBS MEP. Although not shown here, employing an expression similar to Eq. (E1) but using cc-pVTZ and cc-pVQZ bases, yields a method correction, M2, that is essentially identical to M1.

Figure 2(b) reveals the effect of the method correction on the calculated CBS limit MEP for CASPT2, MRCI, and MRCI+Q calculations. The closer agreement between the three solid lines

indicates that the method correction provides a more consistent description of the MEP. After the method correction, the maximum difference between the MRCI+Q and CASPT2 MEP energies is only 25%.

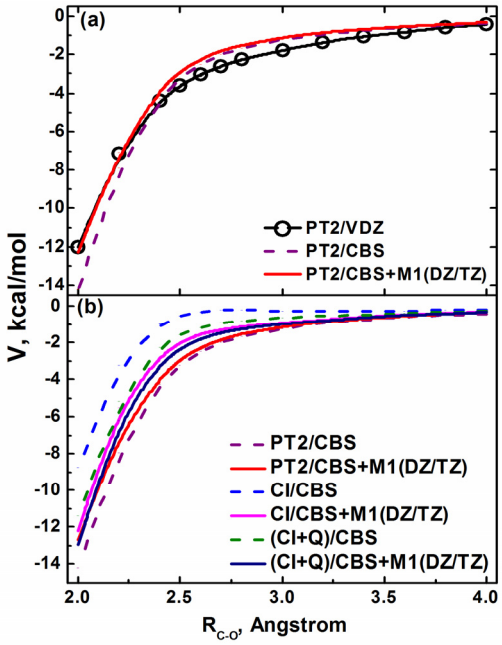

Fig. 2 MEP energies for the phenyl + O_2 reaction from different corrections. PT2 refers to CASPT2, CI refers to MRCI, while M1 represents the method correction evaluated from Eq. (E1).

Figure 3 illustrates the present VRC-TST predictions for the phenyl + O_2 high pressure recombination rate coefficient. The black solid and dash lines illustrate our two best results. They include the CBS, relaxation, and M2 method correction and differ only in whether the CBS and method corrections are evaluated with CASPT2 or MRCI+Q calculations. The difference between the two provides some indication of the uncertainty in our predictions. At room temperature, the nearly factor of two difference is due to the strong sensitivity of the predicted rate to the energetics at R_{CO} ~2.5 Å. Above 1000 K the two results are in much improved agreement, differing by less than a factor of 1.35. In comparing with experiment we take the average of these two predictions as our best prediction.

The blue line with circles illustrates the results obtained when all correction terms are ignored.

At room temperature this reference result is nearly 3 times larger than the best results. But by 1000 K the reference and fully corrected results are within about 20%. The uncertainty in our predictions is smaller when these results agree, because the error arising from the 1-dimensional assumptions implicit in the corrections should then be less important. When only the basis set and relaxation correction are included (pink solid line) the rate constants are overestimated by up to 30% compared with those including the method correction.

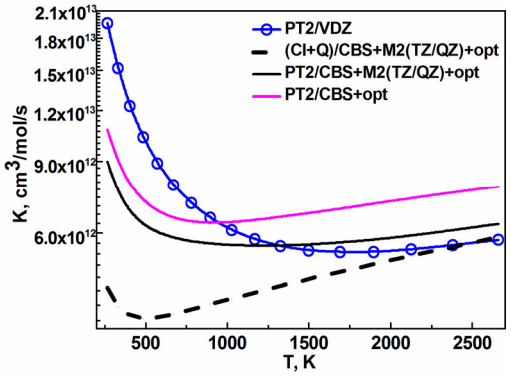

Fig. 3 VRC-TST predicted recombination rate constants for phenyl + O_2.

The computed rate constants show a relatively modest temperature dependence, with first a negative T dependence for T < 900 K, and then a positive T dependence for higher T. This minimum in the rate constant is indicative of the delicate balance between entropic and enthalpic effects. For both T ranges, the transition state is moving to shorter separations with increasing temperature and entropic changes correlate with a negative T dependence, while enthalpic changes correlate with a positive T dependence. At low temperature, the transition state lies at large separation, where the MEP has a small slope and the decreasing entropy dominates the T dependence. At higher T, the transition state lies at shorter separation where the MEP has a larger slope and the enthalpic changes dominate the T dependence.

Our best prediction for phenyl + O_2 is compared with previously reported experimental and

theoretical rate constants in Fig. 4. The VRC-TST predictions are seen to be in good agreement with Yu et al.'s measurements with the CRD technique, and even accurately reproduce the observed negative temperature dependence [10]. In contrast, there is a clear discrepancy between the present VRC-TST predictions and the observation by Schaugg et al. in their fast flow reactor, which shows a positive T dependence over the T range of 418-815 K at 0.7 mbar [13]. Recently, Tanaka et al. also studied this association reaction with the CRD method, measuring the rate coefficient at 296 K and 30 Torr [31], which is in good agreement with our predictions and with the measurements of Yu et al. [10]. The VTST results of da Silva et al. [16], which are based on a G3B3 scaled O3LYP/6-31G(d) PES, are in reasonable agreement with the present predictions, differing by a factor of 2 or less. However, they do show a stronger negative temperature dependence and fail to predict the slightly positive temperature dependence at high temperature. Very recently, Kislov et al. employed VRC-TST to compute the rate constant at high temperatures (1500-2500 K) [18,32]. Their results, which are based on an approximate representation of the transitional mode potential from fits to CASPT2(19,14)//CASSCF(9,9)/aug-cc-pVDZ evaluations, are ~3.5 times greater than ours and show a stronger temperature dependence.

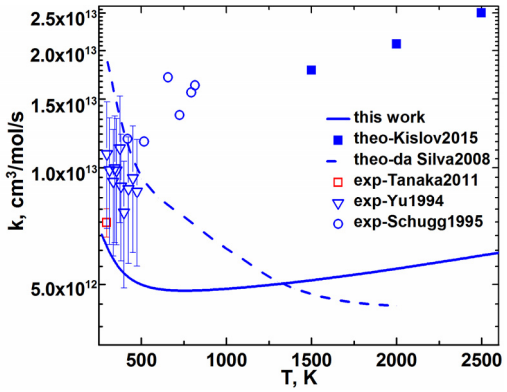

Fig. 4 Comparison between our best prediction and previously reported rate constants for phenyl + O_2 recombination.

3.3 1- and 2-naphthyl + O_2

Figure 5 provides a comparison of the MEP for O_2 adding to 1- and 2-naphthyl. The potential energy has been corrected by all three terms, with Eq. (E1) employed for the method correction. 1-$C_{10}H_7OO$-L and 1-$C_{10}H_7OO$-R are distinguished by the orientation of the –OO group, as indicated by Fig. 1. As expected, the potential energy for 1-$C_{10}H_7OO$-R is very similar to that for 2-$C_{10}H_7OO$. In contrast, there are considerably greater steric interactions with nearby H atoms for 1-$C_{10}H_7OO$-L, which is up to 2.5 kcal/mol more repulsive than 1-$C_{10}H_7OO$-R in the R_{CO} range of 2-4 Å.

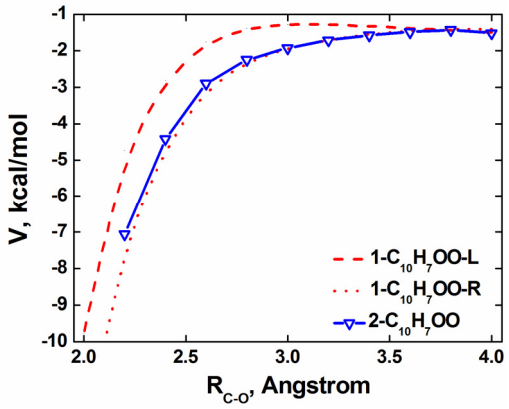

Fig. 5 MEP for 1-$C_{10}H_7$ + O_2 and 2-$C_{10}H_7$ + O_2.

The present predictions for the high pressure recombination rates for naphthyl + O_2 are illustrated in Fig. 6 together with previously reported data, including for phenyl + O_2. The present calculations suggest that the rate constant for adding to 1-naphthyl is about 1.5 times lower than that for adding to phenyl. This is expected on the basis of the increased steric repulsion for 1-naphthyl. In contrast, the predicted rate constant for adding to 2-naphthyl is somewhat greater than that for adding to phenyl. The predicted modest decrease with increasing temperature is again in reasonable accord with the experiments of Park et al. [10,12]. However, the experimental data suggest that O_2 addition to 2-naphthyl should actually be slower than to phenyl (by about a factor of 2) for temperatures in

the 299-444 K range. The reason for this discordance is not clear. It is perhaps worth noting that the theoretical analysis of Kislov also predicts a modest increase in the rate constant from phenyl to 2-naphthyl. However, their rate predictions are again about 3 times higher than the present ones.

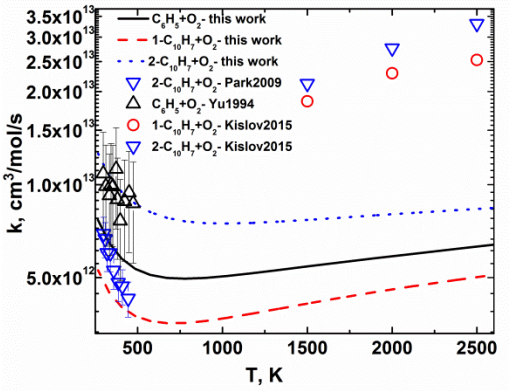

Fig. 6 Comparison between VRC-TST rate constants and previous studies for $C_6H_5 + O_2$, $1\text{-}C_{10}H_7 + O_2$, and $2\text{-}C_{10}H_7 + O_2$.

3.4 Benzyl + O_2

The present kinetic analysis for benzyl radical focuses on the formation of the $C_7H_7O_2$-1 radical since additions to the radical site for the two other resonance structures of C_7H_7 are endothermic (cf., Fig. 1). Figure 7 illustrates the MEP for formation of $C_7H_7O_2$-1 in a *trans* conformation in C_s symmetry at various levels. Notably, due to the resonance stabilization in the C_7H_7 radical, which must be broken before the radical-O_2 bond is formed, the MEP is significantly less attractive than it is for phenyl. Indeed, for most methods there is even a saddle point at about R_{CO} = 2.3 Å.

The MEP curves from the CASPT2(7e,5o), CASPT2(13e,11o), and MRCI+Q calculations are again more consistent after the method correction is included. However, there is still considerable variation in the predicted MEP potential curves even after including the method correction. For example, the CASPT2(7e, 5o) and CASPT2(13e, 11o) predicted saddle points differ by 0.9 kcal/mol. The MRCI+Q MEP is intermediate in value, and might be expected to best handle the effects of

resonance stabilization of the radical.

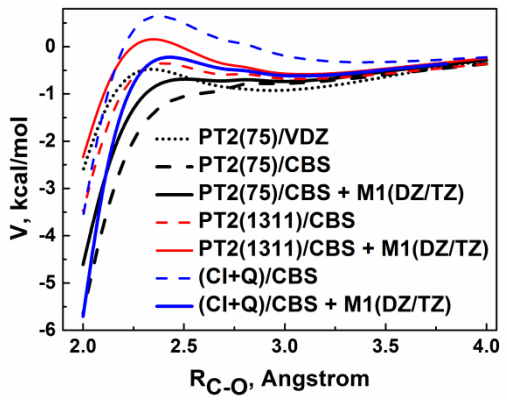

Fig. 7 Potential energy curves for benzyl + O_2 at various levels. PT2(75) refers to the CASPT2(7e,5o) method, PT2(1311) refers to the CASPT2(13e,11o) method, and (CI+Q) refers to MRCI+Q(7e,5o) energies.

Figure 8 presents a comparison of our VRC-TST predictions for the benzyl + O_2 high pressure recombination rate constant with previous experimental measurements [11,14,33,34]. Fenter et al. found the reaction to be independent of pressure in the T range of 298- 398 K, for pressures of 20 and 760 Torr [11]. Hoyermann et al. studied this reaction at low temperature (243–373 K) and somewhat lower pressures (0.8-3 Torr) [14]. The two measured rate constants are within a factor of 2, with Fenter et al.'s results showing a slightly negative temperature dependence, whereas the data of Hoyermann et al. is temperature independent [11,14]. Elmaimouni et al. studied this reaction between 393 and 433 K at 1 Torr [33], showing negative temperature dependence but lower rate coefficients. Nelson et al. reported both temperature and pressure independent rate coefficients in the T range of 295 – 372 K and pressure range of 3-15 Torr [15].

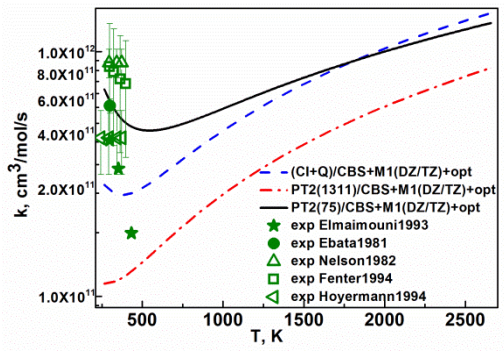

Fig. 8 Comparisons of the VRC-TST predicted recombination rate constants and previous experimental measurements for benzyl + O_2.

The present MRCI+Q based predictions, which are expected to provide the best results, are in reasonably satisfactory agreement with the experimental data. They show a very modest minimum in the rate constant near 400 K and the decline from room temperature to 400 K is in reasonable accord with experiment. Near room temperature the CASPT2(7e,5o) and CASPT2(13e,11o) predictions are about a factor of two higher and lower, respectively. With increasing temperature the discrepancy between the three predictions decreases somewhat. The discrepancy between these predictions roughly correlates with the overall uncertainty in our best prediction for this reaction.

4. Conclusions

The high pressure recombination kinetics for O_2 adding to a series of prototypical aromatic hydrocarbon radicals was studied with direct CASPT2 based VRC-TST theory. The predictions for phenyl, benzyl, 1- and 2-naphthyl radicals over the 300 to 2500 K temperature range are accurately reproduced by the modified Arrhenius expressions reported in the Supplementary material. The predicted kinetics for C_6H_5, 1-$C_{10}H_7$, and 2-$C_{10}H_7$ are fairly similar, with the rates being lowest for 1-$C_{10}H_7$ due to a modest steric effect. In contrast, the resonantly-stabilized character of the benzyl radical leads to much lower reaction enthalpies and rate coefficients.

For the O_2 addition to C_6H_5, 1-$C_{10}H_7$, and 2-$C_{10}H_7$, the calculations predict a modest negative temperature dependence near room temperature, then show a minimum near 600 K, and finally rise by up to a factor of 2 by 2500 K. The predicted temperature dependence for the rate constants is in excellent agreement with many of the experimental observations, which are generally limited to temperatures of 500 K and lower. The predicted magnitudes are in satisfactory agreement with

experiment, with maximum discrepancies within 50%. The resonantly-stabilized benzyl radical is more difficult to treat accurately, especially near room temperature where the predictions are sensitive to the predicted saddle point energy. Nevertheless, our best predictions for benzyl are still in reasonable agreement with experiment. The present systematic kinetic studies for the oxidation of these four typical aromatic radicals enhances our understanding of the structure-activity relationship for such reactions, and should help to improve the rate rules for R + O_2 reactions.

Acknowledgements

This material is based in part on work at Argonne supported by the U.S. Department of Energy, Office of Science, Office of Basic Energy Sciences, Division of Chemical Sciences, Geosciences, and Biosciences under Contract No. DE-AC02-06CH11357. This work is also financially supported by National Natural Science Foundation of China under grants 21303173 and 51376170. We gratefully acknowledge numerous constructive discussions with Yuri Georgievskii and Lawrence B. Harding.

References

[1] T.E. Kleindienst, M. Jaoui, M. Lewandowski, J.H. Offenberg, K.S. Docherty, Atmos. Chem. Phys. 12 (2012) 8711-8726.

[2] J.H. Offenberg, C.W. Lewis, M. Lewandowski, M. Jaoui, T.E. Kleindienst, E.O. Edney, Environ. Sci. Technol. 41 (2007) 3972-3976.

[3] L. Vereecken, J.S. Francisco, Chem. Soc. Rev. 41 (2012) 6259-6293.

[4] J. Zádor, C.A. Taatjes, R.X. Fernandes, Prog. Energy Combust. Sci. 37 (2011) 371-421.

[5] D.R. Glowacki, M.J. Pilling, ChemPhysChem 11 (2010) 3836-3843.

[6] J.G. Calvert, R. Atkinson, K.H. Becker, R.M. Kamens, J.H. Seinfeld, T.J. Wallington, G. Yarwood, The Mechanisms of Atmospheric Oxidation of Aromatic Hydrocarbons, Eds.; Oxford University Press: Oxford, UK,2002.

[7] W. Yuan, Y. Li, P. Dagaut, J. Yang, F. Qi, Combust. Flame 162 (2015) 22-40.

[8] C. Saggese, A. Frassoldati, A. Cuoci, T. Faravelli, E. Ranzi, Combust. Flame 160 (2013) 1168-1190.

[9] F. Battin-Leclerc, Progress in Energy and Combustion Science 34 (2008) 440-498.

[10] T. Yu, M.C. Lin, JACS 116 (1994) 9571-9576.

[11] F.F. Fenter, B. Nozière, F. Caralp, R. Lesclaux, Int. J. Chem. Kinet. 26 (1994) 171-189.

[12] J. Park, Z.F. Xu, M.C. Lin, J. Phys. Chem. A 113 (2009) 5348-5354.

[13] J. Schaugg, R.S. Tranter, H.-H. Grotheer, Rate Coefficients for the Fast Reactions of Phenyl Radicals with NO and O2 from Mass Spectrometric Measurements of Phenyl Decays, Transport phenomena in combustion, Washington, D., Ed., Taylor &Francis ,1996, p.130.

[14] K. Hoyermann, J. Seeba, Proc. Combust. Inst. 25 (1994) 851-858.

[15] H.H. Nelson, J.R. McDonald, J. Phys. Chem. 86 (1982) 1242-1244.

[16] G. da Silva, J.W. Bozzelli, J. Phys. Chem. A 112 (2008) 3566-3575.

[17] Y. Georgievskii, S.J. Klippenstein, J. Phys. Chem. A 107 (2003) 9776-9781.

[18] V.V. Kislov, R.I. Singh, D.E. Edwards, A.M. Mebel, M. Frenklach, Proc. Combust. Inst. 35 (2015) 1861-1869.

[19] C.F. Goldsmith, L.B. Harding, Y. Georgievskii, J.A. Miller, S.J. Klippenstein, J. Phys. Chem. A 119 (2015) 7766-7779.

[20] C.P. Moradi, A.M. Morrison, S.J. Klippenstein, C.F. Goldsmith, G.E. Douberly, J. Phys. Chem. A 117 (2013) 13626-13635.

[21] Y. Georgievskii, S.J. Klippenstein, unpublished.

[22] K. Andersson, P.Å. Malmqvist, B.O. Roos, J. Chem. Phys. 96 (1992) 1218-1226.

[23] G. Ghigo, B.O. Roos, P.-Å. Malmqvist, Chem. Phys. Lett. 396 (2004) 142-149.

[24] J.M.L. Martin, O. Uzan, Chem. Phys. Lett. 282 (1998) 16-24.

[25] G. Knizia, T.B. Adler, H.-J. Werner, J. Chem. Phys. 130 (2009) 054104.

[26] T.B. Adler, G. Knizia, H.-J. Werner, J. Chem. Phys. 127 (2007) 221106.

[27] F.R. Manby, H.-J. Werner, T.B. Adler, A.J. May, J. Chem. Phys. 124 (2006) 094103.

[28] L. Goerigk, S. Grimme, Phys. Chem. Chem. Phys. 13 (2011) 6670-6688.

[29] M.J. Frisch, G.W. Trucks, H.B. Schlegel, G.E. Scuseria, M.A. Robb, Gaussian 09, Revision B.01, Gaussian Inc., Wallingford, CT (2009).

[30] H.J. Werner, P.J. Knowles, G. Knizia, F.R. Manby, M. Schutz, MOLPRO, version 2010.1; www.molpro.net.

[31] K. Tanaka, M. Ando, Y. Sakamoto, K. Tonokura, Int. J. Chem. Kinet. 44 (2012) 41-50.

[32] S.J. Klippenstein, A.F. Wagner, R.C. Dunbar, D.M. Wardlaw, S.H. Robertson, Variflex, version 1.0; Argonne National Laboratory: Argonne, IL, (1999).

[33] L. Elmaimouni, R. Minetti, J.P. Sawerysyn, P. Devolder, Int. J. Chem. Kinet. 25 (1993) 399-413.

[34] T. Ebata, K. Obi, I. Tanaka, Chem. Phys. Lett. 77 (1981) 480-483.